Original Article
microRNA-146a-5p affects the inflammatory response and vascular permeability through targeting autophagy related gene 7 (ATG7) via JAK/STAT3 signaling pathway in chronic idiopathic urticaria

Xiao-Qian Zhou, Zhu-Sheng Yang, Wen-Bin Liu, Xiu-Min Yang

Department of Dermatology, Beijing Tongren Hospital, Capital Medical University, Beijing 100730, P. R. China

Abstract: Objective: This study aims to elucidate the underlying mechanism by which microRNA (miR)-146a-5p and its target gene, autophagy related gene 7 (ATG7), affect the inflammatory response and vascular permeability via the Janus kinase/signal transducer and activator of transcription 3 (JAK/STAT3) signaling pathway in chronic idiopathic urticaria (CIU). Methods: 46 patients with CIU were included in this study. An autologous serum skin test and a serum immunoglobulin assay were performed. Expression of ATG7 in skin tissue was measured by immuno-histochemistry. Enzyme-linked immunosorbent assay (ELISA) was utilized to detect the levels of serum inflammatory factors. Dual luciferase reporter assay was used to confirm whether ATG7 was a target gene of miR-146a-5p. Mast cells and human dermal capillary endothelial cells were prepared and divided into six groups: blank, negative control (NC), miR-146a-5p mimic, miR-146a-5p inhibitor, small interfering (si)RNA-ATG7 and miR-146a-5p mimic + siRNA-ATG7. qRT-PCR and western blotting were used to measure relative gene and protein expression levels, respectively. The mast cell degranulation was calculated. The histamine release rate and vascular permeability were also measured. Results: The results demonstrated that, compared with the Control group, the wheal diameter and the expression of ATG7, immunoglobulin (Ig)A, levels of C5a, C3 and C4, erythrocyte sedimentation rate (ESR), C-reactive protein (CRP), white blood cell count (WBC), rheumatoid factor (RF), IL-4, IL-10 and IgE were significantly increased in patients with CIU, and the JAK/STAT3 pathway was activated. However, the expression levels of IgG, IgM, interferon-α (IFN-α) and miR-146a-5p were significantly downregulated in patients with CIU compared with control patients. Luciferase assay confirmed that ATG7 was the target gene of miR-146a-5p. Compared with the blank group, cells transfected with miR-146a-5p mimic, siRNA-ATG7 and miR-146a-5p mimic + siRNA-ATG7 showed a lower rate of degranulation, histamine release and skin vascular permeability, and activation of the JAK/STAT3 pathway was inhibited. Conversely, the inhibition of miR-146a-5p was able to promote mast-cell degranulation and release of histamine, skin vascular permeability and JAK/STAT3 pathway activation. Conclusion: The present study demonstrated that miR-146a-5p could alleviate the inflammatory response and vascular permeability through inhibition of the JAK/STAT3 signaling pathway by targeting ATG7 in CIU. These results suggested that miR-146a-5p may be a potential diagnostic marker and therapeutic target for CIU.

Keywords: microRNA-146a-5p, autophagy related gene 7, JAK/STAT3 signaling pathway, chronic idiopathic urticaria, mast cell, inflammatory response, vascular permeability

Introduction

Chronic urticaria (CU) predominantly refers to the presence of hives that appear on the skin and disappear within 24 h. Depending on the duration of the symptoms, CU can be categorized into acute (less than 6 weeks in duration) or chronic (more than 6 weeks) forms [1, 2]. Foods, drugs, infections, aeroallergens, contact allergens and autoantibodies to the immu-

noglobulin (Ig)E are the main etiological factors that result in the progression of chronic urticaria [3]. Chronic idiopathic urticaria (CIU), as one of the most common subtypes of CU, has unknown causes compared with CU [4]. At the same time, patients who were treated with antihistamine had poor therapeutic effect and the therapeutic modalities had become a key research directions of dermatologist [5]. However, the underlying etiopathogenesis of CIU

remains largely unknown, thus deeper studies about molecular mechanisms of CIU are needed to provide experimental basis for conquering CIU.

MicroRNAs (miRNAs) are endogenous, small, non-coding RNA sequence that can recognize a cluster of target genes which eventually lead to their degradation or translational inhibition [6]. Studies had indicated that microRNAs affect various cellular activities, such as cell development, carcinogenesis and immune response [7-9]. A recent review article summarized the role of miRNAs in various skin diseases, including malignant melanoma, psoriasis, urticaria, toxic epidermal necrolysis, polymyositis/dermatomyositis and scleroderma [10]. Previous study indicated that miR-146a showed lower levels in tissues obtained from chronic inflammatory disease, for instance, atopic eczena patients [11]. Another study also confirmed that miR-146a exerted crucial functions in modulating inflammation in the skin, and delivery of miR-146a mimics into skin could ameliorate inflammation caused by psoriasis, as well as down-regulate the neutrophil infiltration [12]. But whether it could influence the incidence of CIU remains largely unknown. As a target gene of miR-146a-5p, autophagy related gene 7 (ATG7) plays an important role in the formation of autophages [13]. Previous studies focused on its role in cancer formation and progression [14-16]. Another study designed by Qiang L et al. revealed that ATG7 exerted effects on ultraviolet radiation induced inflammation, and ATG7 deletion could suppress the inflammatory microenvironment and skin tumorigenesis [17]. Previous study had indicated that JAK/STAT3 signaling pathway could affect the development of chronic autoimmune urticaria (CAU), and its inactivation could suppress the pathogenesis of CAU [18]. Based on the above knowledge, the present study hypothesized that miR-146a-5p may serve an important role in CIU through targeting ATG7 via the JAK/STAT3 signaling pathway and hope to provide a diagnostic marker and therapeutic target for CIU.

Materials and methods

Ethic statements

The study was in strict accordance with the Helsinki Declaration and it was approved by the Ethics Committee of Beijing Tongren Hospital, Capital Medical University. Informed consent forms were obtained from all the individuals enrolled in this study.

Study population

A total of 46 patients diagnosed with CIU from January 2016 to December 2017 in Beijing Tongren Hospital, Capital Medical University (Beijing, China), were enrolled in the study. The study group consisted of 14 males and 32 females, and the mean age of the patients was 38.95±11.75 (14-58 years old). The inclusion criteria were as follows: Presence of urticaria symptoms for ≥ 6 weeks, frequency of the wheal was above 3 time; Patients who were at the active phase of CIU; Patients that had the willingness to accept an autologous serum skin test. The exclusion criteria included: Patients with specific etiology such as food, drug, bad living habit; pregnant or lactating women; Patients with serious immune system disorders and primary diseases of the liver, kidney, hematopoietic systems and cardio-cerebral blood vessel; Patients had a systematic use of anti-histamine, glucocorticoid, anticoagulant or immunosuppressants. 46 healthy subjects (18 male and 28 female) were included as a control group, with an average age of 36.95±10.43 (17-56 years old), and people with allergic diseases, or autoimmune diseases were excluded.

Autologous serum skin test

A total of 3 ml peripheral venous blood was collected from subjects, the serum was then separated by centrifugation at 1500 r/min for 10 min at 4°C. 50 μL autologous serum and the same amount of normal saline were separately prepared and intradermally injected into the forearm with injection sites spaced above 5 cm. The results of wheal reaction were evaluated after 30 min. A black marker was used to indicate the wheal line, the longest diameter and its midpoint vertical diameter (d1 and d2) were measured. The final wheal diameter = (d1 + d2)/2 [19].

Serum immunoglobulins test

2 mL serum was separated from venous blood by centrifugation at 1500 r/min for 10 min. Subsequently, immunoglobulin assay kit for IgA

(BMS2096), IgG (BMS2091) and IgM (88-50620-22) (Thermo Fisher, California, USA) was used to detect the serum immunoglobulin levels of IgA, IgG and IgM. The serum levels of IgG, IgM and IgA in the CIU group and the control group were measured using an array 360 specific protein analyzer (Beckman, California, USA).

Immunohistochemistry

Skin tissues were obtained from patients' legs or arms and fixed with 4% paraformaldehyde for 24 h and dehydrated in a graded ethanol series (80, 90 and 100%). The tissues were immersed in paraffin for 30 min for embedding, sliced into 5-μm slices, unfolded at 45°C for 2 min, dehydrated in gradient alcohol (70%, 80%, 90% and 100%) for three times and de-waxed in xylene following baking for 1 h at 60°C. The slices were dehydrated with gradient alcohol (70%, 80%, 90% and 100%) three times and immersed in 3% H_2O_2 for 10 min. Following washing with distilled water, the slices were put into citrate antigen retrieval solution at 121°C and high pressure for 90 sec, cooling to room temperature and washing three times with PBS for 3 min. Slices were blocked with 100 μl 5% bovine serum albumin (B2064, sigma, USA) at 37°C for 30 min and incubated with 100 μl rabbit anti-ATG7 primary antibody (10 μg/mL, ab53255, Abcam, UK) at 4°C overnight and subsequently washed three times with PBS for 3 min each. The slices were incubated with a horseradish peroxidase (HRP) conjugated goat anti-rabbit secondary antibody (1:1000, ab67-21; Abcam, UK) at 37°C for 30 min and washed three times with PBS for 3 min each. 3,3'-diaminobenzidine (AR1025, Wuhan Boster Biological Technology co. ltd, China) was used to develop color at room temperature for 3 min. Sections were counterstained in hematoxylin for 5 min, washed with running water, soaked in 1% hydrochloric acid for 5 sec and washed under running water for 10 min. Image-Pro Plus image analysis software 6.0 (Media Cybernetics, Inc., Rockville, MD US) was used to measure the mean optical density (OD) of ATG7 positive staining prior to quantitative analysis. Staining intensity (SI) and positive cell proportion (PP) were assessed. SI is classified as 4 grades: 0 for colorless, 1 for light yellow, 2 for brown, and 3 for dark brown. PP was divided into 5 grades: 0 for positive cells <5%, 1 for positive cells <10-25%, 2 for 25-50%, 3 for 51-80%, and 4 for >80%. The comprehensive score is the product of SI and PP; 0 is negative (-), 1 is weak positive (+), 2 is medium positive (++), and more than 3 is strong positive (+++) [20].

Enzyme-linked immunosorbent assay (ELISA)

2 ml serum was separated from venous blood by centrifugation at 1500 r/min for 10 min. Then the ELISAs were performed using ELISA Kits according to the manufacturer's protocol. The dissolved standards (50 μl) and the sample (50 μl) were added into plates and incubated at 37°C for 10 min. After washing three times with PBS for 3 min each, enzyme-bound reactant working solution (50 μl) was added and the plates were incubated in the dark at 37°C for 30 min. Subsequently, stop solution was added, and plates were washed three times and 50 μl substrates were added. The OD value was measured at 450 nm using a Multiskan FC microplate reader (FC, Thermo Fisher, USA). The standardized curve was drawn with the standard concentration as abscissa, and OD value as ordinate. The complement components C5a (ab193695, Abcam, UK), C4 (ab108824, Abcam, UK), C3 (ab108822, Abcam, UK), interleukin (IL)-4 (BMS225HS, Thermo Fisher, USA), IL-10 (EHIL10, Thermo Fisher, USA), C-reactive protein (CRP, BMS288INST, Thermo Fisher, USA), rheumatoid factor (RF, KA1442, Abnova, USA), IgE (BMS2097, Thermo Fisher, USA) and interferon (IFN)-α (ab213479, Abcam, UK) in serum were detected. Automatic ESR analyzer (SHS-3000, Safe Heart, China) and Automatic blood cell analyzer (BC-3000Plus, Mindray, China) were used for detecting erythrocyte sedimentation rate (ESR) and white blood cell count (WBC) respectively.

Dual-luciferase reporter gene assay

A biological prediction website, Targetscan (http://www.targetscan.org/vert_72/), was used to predict the target sites of miR-146a-5p on ATG7 3'UTR, and a Luciferase Reporter Gene Detection Kit (LUC1-1KT, Sigma, USA) was used to verify whether miR-146a-5p targeted ATG7. Artificially synthesized segments of the ATG7 3'UTR were introduced into the pMIR-reporter (AM5795, Thermo Fisher, USA) using the restriction enzyme recognition sites for SpeI and HindIII. The mutation sites of the comple-

mentary sequence in wild-type (WT, 3'UTR sequence: 5'-CCCAUAUAGAAAAGUGUUCUCAA-3') ATG7 were designed and the target segments were inserted into the pMIR-reporter vectors using T4 DNA ligase following restriction enzyme digestion. The correctly identified sequence of the luciferase reporter plasmids, WT and mutant (MUT, 3'UTR sequence: 5'-CC-CAUGCCAGUAAGUGUUCUCAA-3') were co-transfected with miR-146a-5p mimic or NC mimic into 293T cells (SCC-120511, Beijing Solarbio Technology Co., Ltd, China). Specifically, cells were seeded into 20-well plate. The transfection was conducted according to the instructions on LipofectamineTM2000 when confluence of cells was up to 50-60% (Invitrogen Inc., Carlsbad, CA, USA). A and B solution were prepared respectively in two sterile Eppendorf (EP) tube. Among them, the A solution was added with 1 μL lipofectamin 2000 and 50 μL serum-free medium and placed at room temperature for 5 min while the B solution was added with reporter plasmids (20 pmoL) and 50 μL serum-free medium, followed by mixing with these two solutions to compound RNA and liposome and placing at room temperature for 20 min. These methods were also suitable for the treatment of miR-146a-5p mimic and NC mimic. The mixture of A and B was added into cells. And cells were cultured in an incubator with 5% CO_2 at 37°C and had a complete medium change after 48 h. Following 48 h incubation, the cells were collected and lysed, and luciferase reporter gene activity was detected using a Luciferase Reporter Gene Detection Kit and microplate reader (Multiskan MK3, Thermo Fisher, USA). The experiment was repeated 3 times.

Cell culture, grouping, and transfection

Foreskin was obtained during circumcision surgery of 16 children aged 1~8 years, and then a mixed cell suspension was prepared. Briefly, the foreskin was washed with saline and immediately placed into RPMI-1640 culture medium (11875093, Thermo Fisher, USA). This was followed by isolation of subcutaneous tissue and washes with Tyrode solution (YM-S1363, Shanghai Yuanmu Biotechnology Co., Ltd., China). Subsequently, the foreskin was cut into tissue blocks (1 mm²), placed in a culture dish with RPMI-1640 containing 1 mg/ml type I collagenase and 0.5 mg/ml hyaluronidase and incubated at 37°C for 4 h. A dropper was uti-

lized repeatedly to digest the solution and create a suspension, which was filtered to remove tissue fragments and larger cell pellets using a nylon net (300-μm pore size). Following collection of the filtered solution and cooling, the cells were resuspended in RPMI-1640 and incubated at 37°C for 4 h in 5% CO_2 with gentle agitation. The mast cells were identified using 0.2% toluidine blue. Human dermal capillary endothelial cells (HDMECs) were purchased from Shanghai Honsun Biological Technology Co., Ltd. (Shanghai, China) and cultured in RPMI-1640 containing 10% fetal bovine serum (10099141, Thermo Fisher, USA), 100 μg/mL penicillin and 100 U/mL streptomycin.

The transfection groups of HDMECs or mast cells included: i) the blank group, in which cells were untransfected; ii) the negative control (NC) group, in which cells were transfected with NC mimic; iii) the miR-146a-5p mimic group, in which cells were transfected with miR-146a-5p mimic; iv) the miR-146a-5p inhibitor group, in which cells were transfected with miR-146a-5p inhibitor; v) the small interfering (si)RNA-ATG7 group, in which cells were transfected with ATG7-targeting siRNA; and vi) miR-146a-5p mimic + siRNA-ATG7 group, in which cells were transfected with miR-146a-5p mimic and siR-NA-ATG7. The cells were subcultured 1 day prior to transfection and were seeded into a 6-well plate (1 × 10⁶ cells/well). When the cells reached 80% confluency, they were transfected using Lipofectamine® 2000 (11668027, Thermo Fisher, USA), according to the manufacturer's instructions. A and B solutions were prepared respectively in two sterile Eppendorf (EP) tubes. Among them, A solution was added with 1 μL lipofectamin 2000 and 50 μL serum-free medium and placed at room temperature for 5 min. B solution was made up of 250 μl serum-free Opti-MEM (11111044, Thermo Fisher, USA) and dilute 100 ng blank vector, NC mimic, siR-NA-ATG7 (5'-CCAACACACTCGAGTCTTT-3'), miR-146a-5p inhibitor or miR-146a-5p mimic (final concentration 50 nM), followed by gentle mixing and incubation at room temperature for 5 min. The two solutions were mixed and incubated at room temperature for 10 min before addition to the wells. The transfected cells were cultured with 5% CO_2 at 37°C for 5-6 h, then complete medium was replaced, and the cells were used in subsequent experiments following incubation at 37°C for 24 h. And then the cover

slip was removed, washed twice with PBS, fixed with glycerol and examined under a fluorescence microscope (IX71-F22FL/DIC, OLYMPUS, Japan) to measure transfection rate.

Detection of degranulation rate of mast cell

Mast cells were incubated at room temperature for 10 min and observed under an inverted microscope (CK40-F200, Olympas, Japan). Normal and degranulated mast cells were present. Normal mast cells were characterized by their oval or circular morphology, granule-filled cytoplasm and a clear structure; degranulated mast cells were unclear and in disorder. The degranulation rate of mast cells was calculated as follows: Degranulation rate = (number of degranulated mast cells/total number of mast cells) × total number of cells.

Histamine release test

Mast cells were diluted with 1640 medium and added into 24-well plate (10^5 cells/well). A total of 100 μl enzyme-bound reactant and histamine antiserum was added into 24 well-plate, mixed gently and incubated at room temperature for 2 h. The wells were washed three times and patted dry. A total of 200 μl 3, 3', 5, 5'-tetramethylbenzidine (TMB) substrate was added per well, and incubated at room temperature for 30 min, washed three times and patted dry. Subsequently, 50 μl TMB stop solution was added and the OD value was measured at 450 nm using a microplate reader, followed by calculation of histamine content against a standard curve. The final histamine release rate was calculated as follows: Histamine spontaneous release rate = (histamine spontaneous release content/total histamine content) × 100%. Total histamine release rate = (histamine release content of samples/total histamine content) × 100%. Histamine release rate = Total histamine release rate of samples - Histamine spontaneous release rate.

Vascular permeability measurement

HDMECs (10^5 cells/mL) were placed in a double-layer transwell culture dish and cultivated with serum-free 1640 medium. Following 30 min cultivation at 37°C, histamine (50 μmol/l) was added to stimulate the cells for an additional 30 min. Subsequently, 1 g/L fluorescein isothiocyanate-dextran was added to cells in the upper layer and cells were cultured at 37°C for 30 min. A total of 50 μl supernatant was collected from each upper layer and fluorescence intensity was measured at 490 nm using a spectrophotometer. The permeability change was shown by fluorescence intensity.

Reverse transcription-quantitative polymerase chain reaction (RT-qPCR)

Liquid nitrogen was added to 100 mg tissues, which were ground until they represented fine powder. Total RNA was extracted from the tissues using TRIzol® (15596026, Thermo Fisher, USA). Ultraviolet spectroscopy (912A0883, Thermo Fisher, USA) was used to examine the purity and RNA concentration of the tissue. Samples with a concentration (A260/A280 = 1.8~2.0) was adopted for the subsequent experiments. RNA was reverse transcribed into cDNA using the PrimeScript RT Reagent kit (DRR047A, Takara, Japan), according to the manufacturer's protocol. The reaction conditions included reverse transcription at 37°C for 15 min and enzyme deactivation at 85°C for 5 sec, frozen at -80°C. The cDNA was diluted with 60 μl DEPC water. qPCR was performed according to the instructions of the SYBR Premix *Ex Taq* II reference kit (RR820A, Takara, Japan). The PCR reaction system included 25 μl SYBR Premix *Ex Taq* II, 2 μl forward and reverse primers, l μl ROX Reference Dye (50 ×), 4 μl cDNA template and 16 μl distilled H_2O. qPCR was performed using an ABI 7500 system (ABI, USA) and the thermocycling conditions were as follows: Initial denaturation at 95°C for 30 sec, followed by 40 cycles of denaturation at 94°C for 20 sec, annealing at 58°C for 30 sec and extension at 72°C for 30 sec. The internal reference for miR-146a-5p was U6 and for other genes was GAPDH. All the primers employed in this study are shown in **Table 1**. $2^{-\Delta\Delta CT}$ was used to represent the relation of target gene expression between the experimental group and the control group: $\Delta\Delta CT = \Delta Ct_{experimental\ group} - \Delta Ct_{control\ group}$, and Ct were cycles when real-time fluorescence intensity reached pre-set threshold value and amplification was at logarithmic growth. All experiments were repeated 3 times.

Western blotting

Liquid nitrogen was added to 200 mg tissues, which were ground until they became fine powder, then 1 mL lysis buffer (AI004-L, Beijing

Table 1. Primer sequences for reverse transcription-quantitative polymerase chain reaction

	Primer sequences (5'(-3')
miR-146a-5p	F: TCGAAAGCTTACCAGGCTTTTCACTCTTGT
	R: TCGAGGATCCGCCTTCTGTCTCCAGTCTTCC
ATG7	F: CCTGCCCTACTTCTTATTC
	R: CAGAGGACTTCAACGGAC
JAK2	F: AGATGTGCCGCTATGACC
	R: CTCTTCCGTGCTGTGCTG
STAT3	F: TATCTTGGCCCTTTGGAATG
	R: GTGGGGATACCAGGATGTTG
IL-4	F: GAGCCATATCCACGCATGCGACAAA
	R: CATGGTGGCACTATGCTACGAGTA
IFN-γ	F: CACTCGACCTTAATCTA
	R: CTCTTGATTCAATGCTTCA
U6	F: GCGCGTCGTGAAGCGTTC
	R: GTGCAGGGTCCGAGGT
GAPDH	F: CGGAGTCAACGGATTTGGTCGTAT
	R: AGCCTTCTCCATGGTGGTGAAGAC

F, forward; miR-146a-5p, microRNA-146a-5p; ATG7, autophagy related gene 7; JAK2, Janus kinase 2; STAT3, signal transducer and activator of transcription 3; IL-4, interleukin-4; IFN-γ, interferon γ; R, reverse.

Qbioscience biological technology Co., LTD, China) was added. The tissues were lysed at 4°C for 60 min and shaken every 10 min. The supernatants were obtained for further use following centrifugation at 1200 r/min at 4°C for 20 min. The protein concentration of each sample was determined using a BCA kit (P0012S, Beyotime Biotechnology, China) and the deionized H_2O was used to adjust concentrations to ensure the consistency. Protein samples were denatured by mixing sample buffer with loading buffer and boiling for 5 min at 100°C. Proteins (30 µg) were loaded into each well and separated by 10% SDS-PAGE, with 4% spacer gel. The proteins were transferred to a nitrocellulose membrane, blocked with 5% non-fat dry milk, and incubated at 4°C overnight with rabbit polyclonal antibodies against ATG7 (1: 20000; ab133528; Abcam, UK), JAK2 (1:1000, ab39636, Abcam, UK), p-JAK2 (1:5000, ab32-101, Abcam, UK), STAT3 (1:5000, ab109085, Abcam, UK), p-STAT3 (1:10000, ab76315, Abcam, UK), IL-4 (0.2 µg/mL, ab9622, Abcam, UK) and IFN-γ (1 µg/ml, ab77246, Abcam, UK) and washed 3 times with PBS at room temperature for 5 min. Horseradish peroxidase-labeled goat anti-rabbit IgG secondary antibody (1: 1000, ab6721, Abcam, UK) was added and the

membranes were incubated for 30 min at 37°C and washed 3 times with PBS for 3 min. Membranes were immersed in Enhanced Chemiluminescence reagents (PE0010, Beijing Solarbio Technology Co., Ltd, China) at room temperature for 2 min, then removed from the solution and covered with plastic wraps. This was followed by X-ray film tableting, developing, fixing and data analysis in the dark. Densitometric analysis of the target protein was normalized with the GAPDH loading control and presented as relative protein content. Image-Pro plus 6.0 (Media Cybernetics, USA) software was used to analyze the gray value of the bands. The above method is also applicable to cell protein extraction.

Statistical analysis

All data were analyzed using SPSS 22.0 software (IBM Corp., Armonk, NY, USA). Enumeration data were analyzed by χ^2 test and results are presented as the mean ± standard deviation. All experiments were repeated ≥ 3 times. Comparisons between two groups were analyzed using t-test, whereas comparisons among multiple groups were performed using one-way analysis of variance followed by Tukey's test. The Kolmogorov-Smirnov method was adopted for nonparametric data. Skew distributional data were analyzed using the post-hoc tests of Dunn in the Kruskal-Wallis test. $P < 0.05$ was considered to indicate a statistically significant difference.

Results

Wheal diameter is greater in CIU patients

As shown in **Figure 1**, the mean wheal diameter was measured and the results demonstrated that the wheal diameter of the serum skin test in the CIU group was significantly larger compared with that in the control group ($P < 0.05$). The wheal diameter of the normal saline skin test in the CIU group was also significantly larger compared with that of the control group ($P < 0.05$). Furthermore, the wheal diameter of the serum skin test was significantly larger compared with the wheal diameter of the normal saline skin test in the CIU group ($P < 0.05$). The results suggested that there is a stronger allergic reaction in CIU patients.
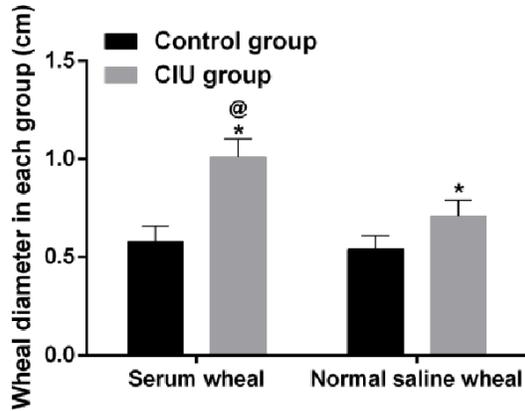
Figure 1. Comparison of two types of wheal diameter in the control group and CIU group. Note: *, compared with control, $P<0.05$, @, compared with normal saline wheal, $P<0.05$.
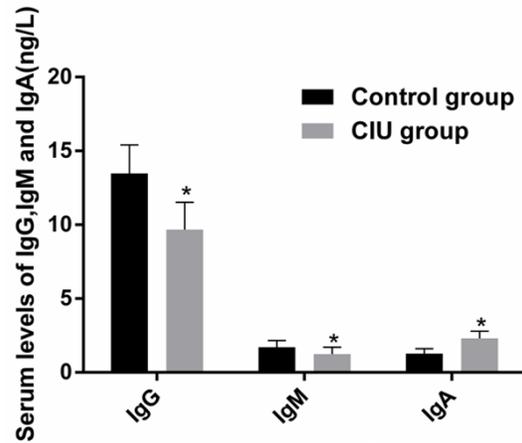
Figure 2. Serum levels of IgG, IgM and IgA in the control group and CIU group. Note: *, compared with the control group, $P<0.05$.

IgA levels was increased while levels of IgG, IgM was decreased in CIU group

The levels of the serum immunoglobulins IgG, IgM and IgA were examined in the CIU group and control group (**Figure 2**). The CIU group exhibited significantly increased IgA level, but significantly decreased IgG and IgM levels compared with the respective levels in the control group ($P<0.05$). The outcomes showed that IgG and IgM were down-regulated but IgA was up-regulated in CIU.

High expression of ATG7 in the CIU patients

ATG7 expression was examined by immunohistochemical staining (**Figure 3**). The CIU group exhibited a significantly increased ATG7 expression (+++) compared with the control group (+). The level of ATG7 expression was up-regulated in CIU.

Abnormal expression of inflammatory cytokines in patients with CIU

As shown in **Table 2**. Patients in the CIU group exhibited significantly increased expression levels of C5a, C3, C4, IL-4, IL-10, ESR, CRP, WBC, RF and IgE, and a significantly decreased expression level of IFN-α (all $P<0.05$). There was an imbalance expression of inflammatory cytokines in CIU.

miR-146a-5p expression was inhibited while JAK/STAT3 signaling pathway was activated in patients with CIU

Patients in the CIU group exhibited significantly decreased expression levels of miR-146a-5p

compared with patients in the control group ($P<0.05$). However, the CIU group exhibited significantly increased mRNA and protein expression levels of ATG7, JAK2, STAT3, as well as p-JAK2, p-STAT3 protein expression compared with the control group (all $P<0.05$) (**Figure 4**). As a result, miR-146a-5p expression was inhibited but JAK/STAT3 signaling pathway was activated in CIU.

ATG7 is a target of miR-146a-5p

According to the online bioinformatics analysis software available at Targetscan, there is a miR-146a-5p target site on the ATG7 3'UTR (**Figure 5**). A luciferase reporter assay was used to verify whether ATG7 was the target gene of miR-146a-5p. The results demonstrated that the luciferase activity in cells co-transfected with miR-146a-5p mimic + ATG7-WT group was significantly reduced compared with the miR-NC group ($P<0.05$), whereas no significant difference was identified following co-transfection with MUT-3'UTR ($P>0.05$). These results suggested that miR-146a-5p targeted ATG7.

miR-146a-5p overexpression or ATG7 knockdown inhibits degranulation of mast cells

As shown in **Figure 6**, the threshing rates of mast cells in six experimental groups were examined. Compared with the blank group, the miR-146a-5p mimic group, the siRNA-ATG7 group and the miR-146a-5p mimic + siRNA-ATG7 groups all exhibited a significant decrease in threshing rate, whereas the miR-146a-5p inhibitor group exhibited an increased thresh-
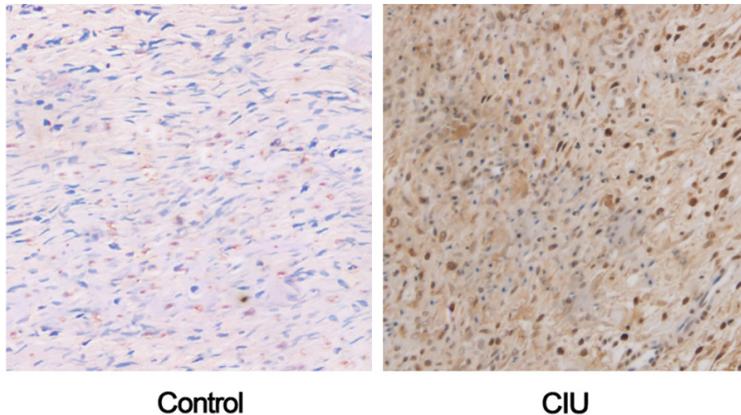
Figure 3. ATG7 expression in the Control group and patients with CIU (× 400).

Table 2. Levels of inflammatory cytokines in serum, as measured by ELISA

Group	Control (n = 46)	CIU (n = 46)	t	P-value
C5a (ng/mL)	18.24±2.59	30.18±0.51	30.68	<0.0001
C4 (g/L)	0.75±0.28	1.67±0.21	17.38	<0.0001
C3 (g/L)	0.28±0.16	0.67±0.19	10.65	<0.0001
IL-4 (ng/mL)	25.36±14.35	35.34±12.21	3.59	0.0005
IL-10 (ng/mL)	3.75±2.03	5.54±3.23	3.18	0.002
ESR (mm/h)	6.63±3.7	12.42±6.49	5.25	<0.0001
CRP (mg/dL)	0.21±0.06	0.68±0.14	20.93	<0.0001
WBC (10^9/L)	5.45±1.22	7.45±3.15	4.01	0.0001
RF (IU/mL)	4.14±0.57	5.62±0.53	12.90	<0.0001
IgE (ng/mL)	39.27±10.33	118.42±41.67	12.50	<0.0001
IFN-α (ng/mL)	12.87±6.57	2.42±1.34	10.57	<0.0001

C5, complement component 5 receptor; C3, complement component 3; C4, complement component 4; IL-4, interleukin 4; IL-10, interleukin 10; ESR, erythrocyte sedimentation rate; CRP, C-reactive protein; WBC, White blood cell count; RF, rheumatoid factor, IgE, immunoglobulin E; IFN-α, interferon α.

ing rate (all P<0.05). There was no significant differences between the blank and the NC groups (P>0.05). Compared with the miR-146a-5p mimic-transfected group and the siRNA-ATG7-transfected group, the miR-146a-5p mimic + siRNA-ATG7-transfected group exhibited a significantly reduced threshing rate (P<0.05). Above results demonstrated that degranulation of mast cells was suppressed by miR-146a-5p overexpression or ATG7 knockdown. And combination of above two treatments had more significant effects on degranulation of mast cells.

miR-146a-5p overexpression or ATG7 knockdown inhibits histamine release by mast cells

Histamine release rate was measured and the results indicated that, compared with the blank group, the miR-146a-5p mimic group, the siRNA-ATG7 group and the miR-146a-5p mimic + siRNA-ATG7 group exhibited significantly reduced histamine release rates, whereas the miR-146a-5p inhibitor group exhibited an increased histamine release rate (all P<0.05) (**Figure 7**). No significant differences were identified between the blank and the NC groups (P>0.05). Compared with the miR-146a-5p mimic group and siRNA-ATG7 group, the miR-146a-5p mimic + siRNA-ATG7 group exhibited a significantly decreased histamine release rate (P<0.05). Results indicated histamine release by mast cells could be inhibited through miR-146a-5p overexpression or ATG7 knockdown, which was apparently suppressed by joint of two above treatments.

miR-146a-5p overexpression or ATG7 knockdown decreases permeability of HDMECs

Spectrophotometry was used to measure the permeability of transfected HDMECs (**Figure 8**). Compared with the blank group, the miR-146a-5p mimic group, the siRNA-ATG7 group and the miR-146a-5p mimic + siRNA-ATG7 group exhibited declined permeability (indicated by increased fluorescence intensity), whereas the miR-146a-5p inhibitor-treated group exhibited increased permeability (indicated by decreased fluorescence intensity) (all P<0.05). No significant differences in permeability were identified between the blank group and the NC group (P>0.05). Compared with the miR-146a-5p mimic group and the si-ATG7 group, the miR-146a-5p mimic + siRNA-ATG7 group exhibited significantly decreased permeability (P<0.05). From above results we can obtain the conclusion that miR-146a-5p overexpression or ATG7 knockdown could decrease vascular permeability which was obviously reduced in miR-146a-5p mimic + siRNA-ATG7 group.
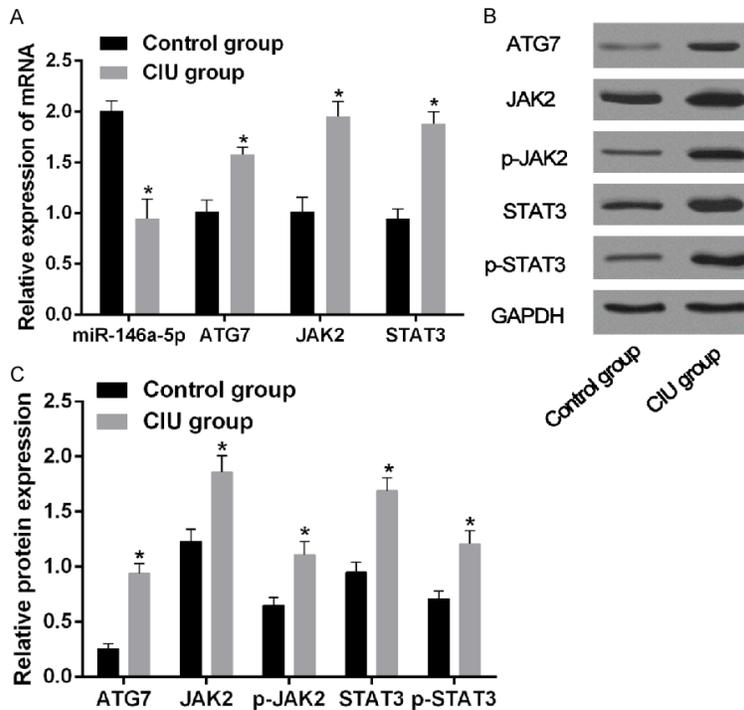
Figure 4. miR-146a-5p expression was inhibited but JAK/STAT3 signaling pathway was activated in CIU. A. miR-146a-5p levels and mRNA expression of JAK/STAT3 pathway related genes. B. Representative western blotting images. C. Quantification of protein expression. *, compared with the control group, *P*<0.05.

miR-146a-5p overexpression or ATG7 knock-down inhibits JAK/STAT3 signaling pathway activation

RT-qPCR and Western blotting were performed to examine the mRNA and protein expression levels, respectively, in treated cells (**Figure 9**). Compared with the blank group, the miR-146a-5p mimic and the miR-146a-5p mimic + siRNA-ATG7 groups exhibited significantly increased miR-146a-5p expression, whereas the miR-146a-5p inhibitor group exhibited a significantly reduced miR-146a-5p expression levels (*P*<0.05); and there was no difference identified in miR-146a-5p expression level in the siRNA-ATG7 group compared with the blank group (*P*>0.05). The miR-146a-5p mimic group, the siRNA-ATG7 group and the miR-146a-5p mimic + siRNA-ATG7 group exhibited significantly reduced mRNA and protein expression levels of ATG7, JAK2, STAT3, IL-4, protein expression of p-JAK2, p-STAT3, and significantly increased in IFN-γ mRNA and protein expression levels compared with the respective expression levels in the blank group (all *P*<0.05). The miR-146a-5p

inhibitor group exhibited an increase in mRNA and protein expression of ATG7, JAK, STAT3 and IL-4, protein expression of p-JAK2, p-STAT3, and significantly reduced IFN-γ mRNA and protein expression levels, compared with the respective expression levels in the blank group (all *P*<0.05). Compared with the miR-146a-5p mimic group and the siRNA-ATG7 group, the miR-146a-5p mimic + siRNA-ATG7 group exhibited reduced mRNA and protein expression levels of ATG7, JAK2, STAT3, IL-4, protein expression of p-JAK2, p-STAT3, and increased in IFN-γ mRNA and protein expression levels (all *P*<0.05). miR-146a-5p overexpression or ATG7 knockdown could repress JAK/STAT3 signaling pathway activation. And combination of above two treatments showed better inhibition.

Discussion

miRNAs have been reported to exert as both biomarkers and possible therapeutic targets in various skin diseases [21, 22]. For instance, previous study indicated that up-regulation of miR-187 could reduce acanthosis and disease severity of psoriasis, suggesting that miR-187 could serve as a potent target in treating psoriasis [23]. It was reported that miR-203 could decrease skin immune responses through inhibiting key pro-inflammatory cytokines [24]. The expression of miR-146 a/b seems to play a significant part in normal function of immune system [25]. Another study also confirmed that miR-146a exhibited specific regulation in psoriasis and could restrain innate immune responses [26, 27]. This study aimed to elucidate the effects of miR-146a-5p and its target gene, ATG7 in pathogenesis of CIU through inhibiting JAK/STAT3 signaling pathway.

First, autologous serum skin test (ASST) was performed to determine the presence of autologous response in patients with CIU and the results indicated that, compared with the control group, the wheal diameter in patients with

A

Position 1708-1714 of ATG7 3' UTR	5'	. . . GAAUGCAGAUGCAGUGUUCUCAU. . .				7mer-A1	-0.02
hsa-miR-146a-5p	3'	UUGGGUACCUUAAGUCAAGAGU				

B
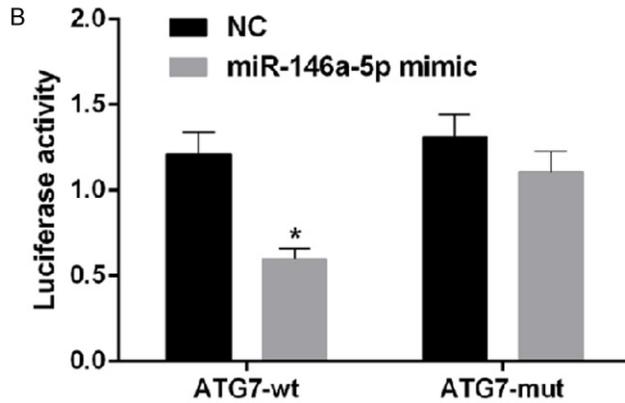
Figure 5. ATG7 is a target gene of miR-146a-5p. A. Predicted target site of miR-146a-5p in the ATG7 3'UTR. B. miR-146a-5p targets ATG7, as determined by the dual-luciferase reporter assay. *, compared with control, $P<0.05$.
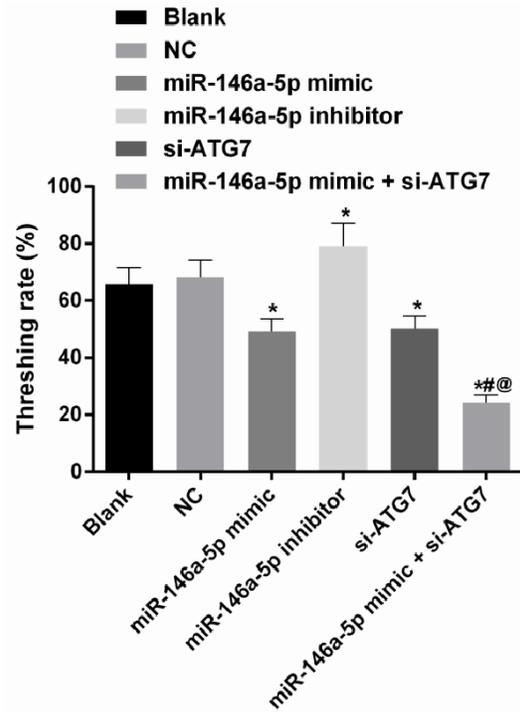
Figure 6. miR-146a-5p overexpression or ATG7 knockdown inhibits degranulation of mast cells. *, compared with control, $P<0.05$; #, compared with miR-146a-5p mimic, $P<0.05$; @, compared with si-ATG7, $P<0.05$.
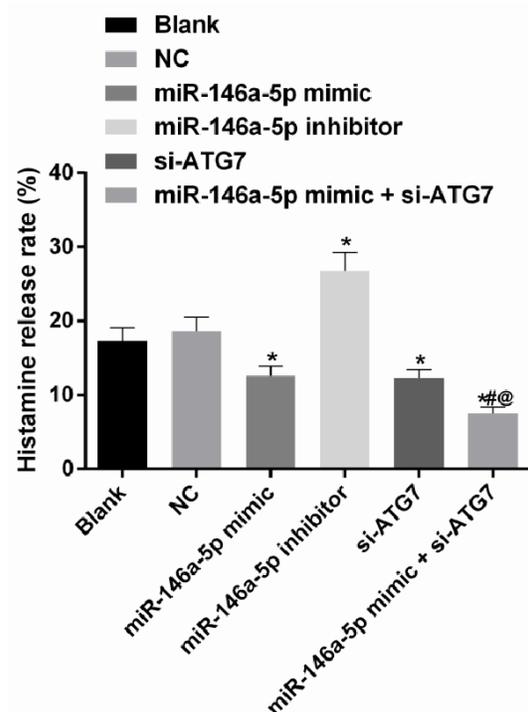
Figure 7. miR-146a-5p overexpression or ATG7 knockdown inhibits histamine release by mast cells. *, compared with control, $P<0.05$; #, compared with miR-146a-5p mimic, $P<0.05$; @, compared with si-ATG7, $P<0.05$.

CIU was significantly increased, suggesting that there was obvious itch in CIU patients, and the CIU patients may need more antihistamine. Immune dysfunction is considered to be an important cause of urticaria [28]. IgM and IgG are the earliest antibodies in the body to respond to basic antigens, and exert crucial importance in the body's anti-infection [29]. At the same time, the imbalance of IgA, IgG and IgM expression was considered to be an impor-
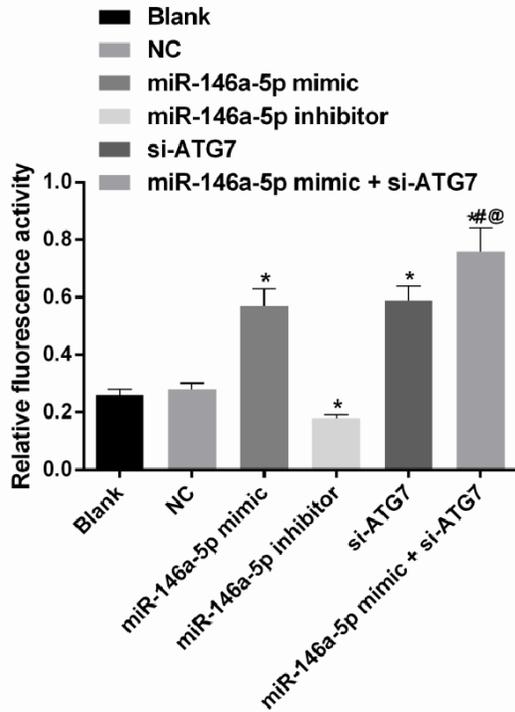
Figure 8. miR-146a-5p overexpression or ATG7 knockdown decreases the permeability of HDMECs. *, compared with control, *P*<0.05; #, compared with miR-146a-5p mimic, *P*<0.05; @, compared with si-ATG7, *P*<0.05.

tant cause of CIU [30]. We further confirmed this conclusion in the present study. Inflammatory factors also play an important role in the pathogenesis of CIU [31]. A large quantity of inflammatory promoters can stimulate the endothelial cells and macrophages and induce the generation of chemokines, subsequently accelerating the activation of T cells and neutrophils, and inducing the pathogenesis of autoimmune diseases [32]. In the present study, the expressions of inflammatory factors in serum of CIU patients were significantly increased except INF-α. It has been reported that the secretion of INF-α was impaired compared with healthy people [33]. By detecting the expression of inflammatory factors in serum and tissues of patients with CIU and control group, we may further confirm the relationship between inflammatory factors imbalance and the pathogenesis of CIU. Upregulation of expression of C5a, C4, C3, IL-4, IL-10, ESR, CRP, WBC, RF, IgE and INF-α inhibition may further aggravate the pathogenesis of CIU.

ATG7 has been reported to have potent antistromal microenvironment inflammation effect, and it can exert its effects on preventing dermal inflammatory reaction and skin tumorigenesis [17]. Results obtained from the immunohistochemistry showed that the positive expression rate of ATG7 in CIU group was significantly higher than that in control group. Furthermore, it was revealed in a targeted relationship prediction website that miR-146a-5p was one of the miRNAs that negatively regulated ATG7, therefore we speculate that miR-146a-5p may affect the morbidity of CIU through the negative regulation of ATG7 and verified this hypothesis by several experiments. JAKs were reported to participate in the pathogenesis of psoriasis, atopic or chronic dermatitis. At the same time, inhibitors of JAK were confirmed as therapeutic candidates in treating chronic dermatitis [34]. Another study also confirmed that using JAK inhibitors was an effective way in treating skin inflammatory disorders by down-regulating activation and differentiation of T cell [35]. In addition, Luo Xiao-Yan et al. indicated that OSMR-gene silencing could restrain the progression of CIU by inhibiting the activation of JAK/STAT3 signaling pathway [18]. The above evidence illustrated the effect of JAK/STAT3 pathway in CIU. Mast cell degranulation and excessive histamine release are important causes of CIU [36]. In the present study, we find that compared with NC group, the release rate of histamine and mast cell exfoliation condition in miR-146a-5p mimic group, siRNA-ATG7 group and miR-146a-5p mimic + siRNA-ATG7 group were significantly decreased, and at the same time, miR-146a-5p mimic + siRNA-ATG7 group exhibited the most obvious decline. Vascular mechanism is confirmed to be an important factor in the pathogenesis of CU [37]. Vascular endothelial cells of CIU patients can be activated by autoantibodies, histamines and mast cell release mediators [38]. At the same time, study of Ren et al. indicated that the expressions of vascular cell adhesion molecule and intercellular adhesion molecule in CU patients were higher than those in normal people, and it may be an important cause of inflammatory response and enhanced vascular permeability in CU patients [39]. Results obtained from the vascular permeability test indicated that overexpression of miR-146a-5p or silencing of ATG7 can reduce the vascular permeability. Results of RT-qPCR and Western blotting showed that miR-146a-5p overexpression or ATG7 silencing can significantly decrease the expression of JAK/STAT3 signaling pathway-related proteins,
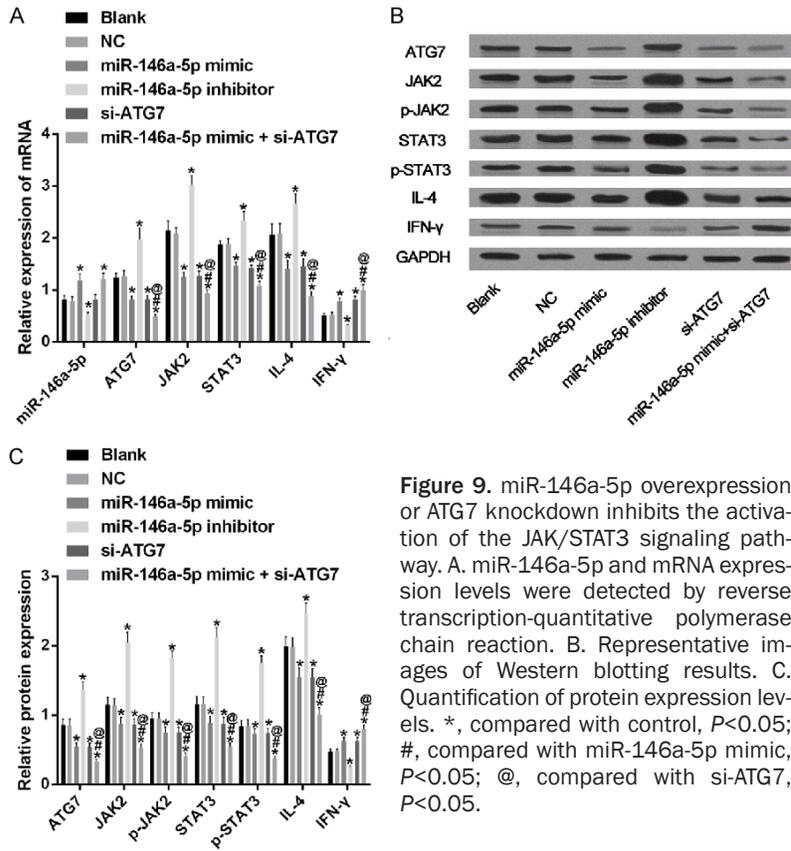
Figure 9. miR-146a-5p overexpression or ATG7 knockdown inhibits the activation of the JAK/STAT3 signaling pathway. A. miR-146a-5p and mRNA expression levels were detected by reverse transcription-quantitative polymerase chain reaction. B. Representative images of Western blotting results. C. Quantification of protein expression levels. *, compared with control, $P<0.05$; #, compared with miR-146a-5p mimic, $P<0.05$; @, compared with si-ATG7, $P<0.05$.

and inhibit the activation of JAK/STAT3 signaling pathway. Thus we speculate that miR-146a-5p regulates the inflammatory response and vascular permeability in CIU patients possibly through the negative regulation of ATG7 and inhibiting the activation of JAK/STAT3 signaling pathway.

In summary, the present study demonstrated the underlying mechanism by which miR-146a-5p affects the inflammatory response and vascular permeability via JAK/STAT3 signaling pathway by targeting ATG7 in CIU. However further research is still required in the future to further elucidate the underlying mechanism of miR-146a-5p in CIU.

Disclosure of conflict of interest

None.

Address correspondence to: Xiu-Min Yang, Department of Dermatology, Beijing Tongren Hospital, Capital Medical University, No. 1 Beijing Legation Quarter, Dongcheng District, Beijing 100730, P. R. China. Tel: +86-010-58268092; E-mail: xiuminyang010@sina.com

References

[1] Nettis E, Cegolon L, Di Leo E, Lodi Rizzini F, Detoraki A and Canonica GW. Omalizumab chronic spontaneous urticaria: efficacy, safety, predictors of treatment outcome, and time to response. Ann Allergy Asthma Immunol 2018; 121: 474-478.

[2] Wang L, Ke X, Kavati A, Wertz D, Huang Q, Willey VJ, Stephenson JJ, Ortiz B, Paknis B, Bernstein JA and Beck LA. Real-world treatment patterns and outcomes of omalizumab use in patients with chronic idiopathic urticaria. Curr Med Res Opin 2018; 34: 35-39.

[3] Sterbank J, Kim Y, Toller-Artis E, Barcena M, Bose S, Meyerson H, Hostoffer R and Tcheurekdjian H. Contemplating the etiology of chronic urticaria and the implications of current guidelines. Ann Allergy Asthma Immunol 2015; 114: 526-527.

[4] Williams P, Kavati A, Pilon D, Xiao Y, Zhdanava M, Balp MM, Lefebvre P, Ortiz B and Hernandez-Trujillo V. Health care burden and treatment patterns in commercially insured children with chronic idiopathic/spontaneous urticaria: a real-world study in the United States. Allergy Asthma Proc 2018; 39: 201-211.

[5] Schmetzer O, Lakin E, Topal FA, Preusse P, Freier D, Church MK and Maurer M. IL-24 is a common and specific autoantigen of IgE in patients with chronic spontaneous urticaria. J Allergy Clin Immunol 2018; 142: 876-882.

[6] Singhvi G, Manchanda P, Krishna Rapalli V, Kumar Dubey S, Gupta G and Dua K. MicroRNAs as biological regulators in skin disorders. Biomed Pharmacother 2018; 108: 996-1004.

[7] Wcislo-Dziadecka D, Simka K, Kazmierczak A, Kruszniewska-Rajs C, Gola J, Grabarek B, Hybiak J, Grillon C, Mazurek U and Los MJ. Psoriasis treatment changes the expression profile of selected caspases and their regulatory microRNAs. Cell Physiol Biochem 2018; 50: 525-537.

[8] Yan JJ, Qiao M, Li RH, Zhao XT, Wang XY and Sun Q. Downregulation of miR-145-5p contributes to hyperproliferation of keratinocytes and

skin inflammation in psoriasis. Br J Dermatol 2019; 180: 365-372.

[9] Sole C, Domingo S, Ferrer B, Moline T, Ordi-Ros J and Cortes-Hernandez J. MicroRNA expression profiling identifies miR-31 and miR-485-3p as regulators in the pathogenesis of discoid cutaneous lupus. J Invest Dermatol 2019; 139: 51-61.

[10] Jinnin M. Recent progress in studies of miRNA and skin diseases. J Dermatol 2015; 42: 551-558.

[11] Sonkoly E, Wei T, Janson PC, Saaf A, Lundeberg L, Tengvall-Linder M, Norstedt G, Alenius H, Homey B, Scheynius A, Stahle M and Pivarcsi A. MicroRNAs: novel regulators involved in the pathogenesis of psoriasis? PLoS One 2007; 2: e610.

[12] Srivastava A, Nikamo P, Lohcharoenkal W, Li D, Meisgen F, Xu Landen N, Stahle M, Pivarcsi A and Sonkoly E. MicroRNA-146a suppresses IL-17-mediated skin inflammation and is genetically associated with psoriasis. J Allergy Clin Immunol 2017; 139: 550-561.

[13] Xia C, He Z, Liang S, Chen R, Xu W, Yang J, Xiao G and Jiang S. Metformin combined with nelfinavir induces SIRT3/mROS-dependent autophagy in human cervical cancer cells and xenograft in nude mice. Eur J Pharmacol 2019; 848: 62-69.

[14] Zhang J, Mao S, Wang L, Zhang W, Zhang Z, Guo Y, Wu Y, Yi F and Yao X. MicroRNA154 functions as a tumor suppressor in bladder cancer by directly targeting ATG7. Oncol Rep 2019; 41: 819-828.

[15] Wu C, Yang L, Qi X, Wang T, Li M and Xu K. Inhibition of long non-coding RNA HOTAIR enhances radiosensitivity via regulating autophagy in pancreatic cancer. Cancer Manag Res 2018; 10: 5261-5271.

[16] Classen F, Kranz P, Riffkin H, Pompsch M, Wolf A, Gopelt K, Baumann M, Baumann J, Brockmeier U and Metzen E. Autophagy induced by ionizing radiation promotes cell death over survival in human colorectal cancer cells. Exp Cell Res 2019; 374: 29-37.

[17] Qiang L, Sample A, Shea CR, Soltani K, Macleod KF and He YY. Autophagy gene ATG7 regulates ultraviolet radiation-induced inflammation and skin tumorigenesis. Autophagy 2017; 13: 2086-2103.

[18] Luo XY, Liu Q, Yang H, Tan Q, Gan LQ, Ren FL and Wang H. OSMR gene effect on the pathogenesis of chronic autoimmune Urticaria via the JAK/STAT3 pathway. Mol Med 2018; 24: 28.

[19] Sabroe RA, Grattan CE, Francis DM, Barr RM, Kobza Black A and Greaves MW. The autologous serum skin test: a screening test for autoantibodies in chronic idiopathic urticaria. Br J Dermatol 1999; 140: 446-452.

[20] Konno R, Yamakawa H, Utsunomiya H, Ito K, Sato S and Yajima A. Expression of survivin and Bcl-2 in the normal human endometrium. Mol Hum Reprod 2000; 6: 529-534.

[21] Feng SJ, Chu RQ, Ma J, Wang ZX, Zhang GJ, Yang XF, Song Z and Ma YY. MicroRNA138 regulates keratin 17 protein expression to affect HaCaT cell proliferation and apoptosis by targeting hTERT in psoriasis vulgaris. Biomed Pharmacother 2017; 85: 169-176.

[22] Mannucci C, Casciaro M, Minciullo PL, Calapai G, Navarra M and Gangemi S. Involvement of microRNAs in skin disorders: a literature review. Allergy Asthma Proc 2017; 38: 9-15.

[23] Tang L, He S, Zhu Y, Feng B, Su Z, Liu B, Xu F, Wang X, Liu H, Li C, Zhao J, Zheng X, Sun C, Lu C and Zheng G. Downregulated miR-187 contributes to the keratinocytes hyperproliferation in psoriasis. J Cell Physiol 2019; 234: 3661-3674.

[24] Primo MN, Bak RO, Schibler B and Mikkelsen JG. Regulation of pro-inflammatory cytokines TNFalpha and IL24 by microRNA-203 in primary keratinocytes. Cytokine 2012; 60: 741-748.

[25] Ahn J, Lee H, Jung CH, Jeon TI and Ha TY. MicroRNA-146b promotes adipogenesis by suppressing the SIRT1-FOXO1 cascade. EMBO Mol Med 2013; 5: 1602-1612.

[26] Hermann H, Runnel T, Aab A, Baurecht H, Rodriguez E, Magilnick N, Urgard E, Sahmatova L, Prans E, Maslovskaja J, Abram K, Karelson M, Kaldvee B, Reemann P, Haljasorg U, Ruckert B, Wawrzyniak P, Weichenthal M, Mrowietz U, Franke A, Gieger C, Barker J, Trembath R, Tsoi LC, Elder JT, Tkaczyk ER, Kisand K, Peterson P, Kingo K, Boldin M, Weidinger S, Akdis CA and Rebane A. miR-146b probably assists mirna-146a in the suppression of keratinocyte proliferation and inflammatory responses in psoriasis. J Invest Dermatol 2017; 137: 1945-1954.

[27] Shams K, Kurowska-Stolarska M, Schutte F, Burden AD, McKimmie CS and Graham GJ. MicroRNA-146 and cell trauma down-regulate expression of the psoriasis-associated atypical chemokine receptor ACKR2. J Biol Chem 2018; 293: 3003-3012.

[28] Antia C, Baquerizo K, Korman A, Alikhan A and Bernstein JA. Urticaria: a comprehensive review: treatment of chronic urticaria, special populations, and disease outcomes. J Am Acad Dermatol 2018; 79: 617-633.

[29] Raskovic S, Matic IZ, Dordic M, Damjanovic A, Kolundzija B, Grozdanic-Stanisavljevic N, Besu I, Jovicic Z, Bijelic B, Jankovic L and Juranic Z. Immunoreactivity to food antigens in patients with chronic urticaria. Immunol Invest 2014; 43: 504-516.

[30] Cildag S and Senturk T. The effect of omalizumab treatment on IgE and other immuno-

globulin levels in patients with chronic sponta-
neous urticaria and its association with treat-
ment response. Postepy Dermatol Alergol
2018; 35: 516-519.

[31] Grzanka A, Machura E, Misiolek M, Polaniak R,
Kasperski J and Kasperska-Zajac A. Systemic
inflammatory response and calcification mark-
ers in patients with long lasting moderate-se-
vere chronic spontaneous urticaria. Eur J
Dermatol 2015; 25: 26-28.

[32] Raphael I, Nalawade S, Eagar TN and
Forsthuber TG. T cell subsets and their signa-
ture cytokines in autoimmune and inflamma-
tory diseases. Cytokine 2015; 74: 5-17.

[33] Futata E, Azor M, Dos Santos J, Maruta C, Sotto
M, Guedes F, Rivitti E, Duarte A and Sato M.
Impaired IFN-alpha secretion by plasmacytoid
dendritic cells induced by TLR9 activation in
chronic idiopathic urticaria. Br J Dermatol
2011; 164: 1271-1279.

[34] Tanimoto A, Shinozaki Y, Yamamoto Y, Katsuda
Y, Taniai-Riya E, Toyoda K, Kakimoto K, Kimoto
Y, Amano W, Konishi N and Hayashi M. A novel
JAK inhibitor JTE-052 reduces skin inflamma-
tion and ameliorates chronic dermatitis in ro-
dent models: comparison with conventional
therapeutic agents. Exp Dermatol 2018; 27:
22-29.

[35] Amano W, Nakajima S, Yamamoto Y, Tanimoto
A, Matsushita M, Miyachi Y and Kabashima K.
JAK inhibitor JTE-052 regulates contact hyper-
sensitivity by downmodulating T cell activation
and differentiation. J Dermatol Sci 2016; 84:
258-265.

[36] Church MK, Kolkhir P, Metz M and Maurer M.
The role and relevance of mast cells in urticar-
ia. Immunol Rev 2018; 282: 232-247.

[37] Tedeschi A, Asero R, Marzano AV, Lorini M,
Fanoni D, Berti E and Cugno M. Plasma levels
and skin-eosinophil-expression of vascular en-
dothelial growth factor in patients with chronic
urticaria. Allergy 2009; 64: 1616-1622.

[38] Bossi F, Frossi B, Radillo O, Cugno M, Tedeschi
A, Riboldi P, Asero R, Tedesco F and Pucillo C.
Mast cells are critically involved in serum-me-
diated vascular leakage in chronic urticaria
beyond high-affinity IgE receptor stimulation.
Allergy 2011; 66: 1538-1545.

[39] Ren G, Zhao X, Zhang L, Zhang J, L'Huillier A,
Ling W, Roberts AI, Le AD, Shi S, Shao C and
Shi Y. Inflammatory cytokine-induced intercel-
lular adhesion molecule-1 and vascular cell
adhesion molecule-1 in mesenchymal stem
cells are critical for immunosuppression. J
Immunol 2010; 184: 2321-2328.